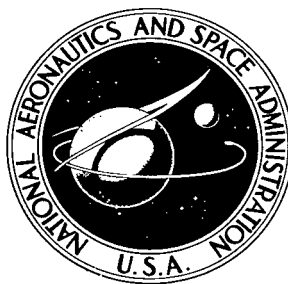


NASA TECHNICAL NOTE



NASA TN D-5382

2.1

NASA TN D-5382



LOAN COPY: RETURN TO
AFWL (WLIL-2)
KIRTLAND AFB, N MEX

SOME LIQUID OXYGEN/LIQUID
HYDROGEN EXPLOSIVE EFFECTS
IN CONTROLLED FAILURE-MODE TESTS

by Richard W. High

Manned Spacecraft Center

Houston, Texas



SOME LIQUID OXYGEN/LIQUID HYDROGEN EXPLOSIVE
EFFECTS IN CONTROLLED FAILURE-MODE TESTS

By Richard W. High

Manned Spacecraft Center
Houston, Texas

NATIONAL AERONAUTICS AND SPACE ADMINISTRATION

For sale by the Clearinghouse for Federal Scientific and Technical Information
Springfield, Virginia 22151 - CFSTI price \$3.00

ABSTRACT

The explosive yield data from three launch vehicle propellants are analyzed and compared. These data from controlled failure-mode tests are found to be proportional to the interface area of contact between the fuel and oxidizer. The comparison of the data at short delay times suggests that, when the interface area of contact is equal, the potential hazard of liquid oxygen/liquid hydrogen is similar to that of liquid oxygen/kerosene and to nitrogen tetroxide/Aerozine-50.

CONTENTS

Section	Page
SUMMARY	1
INTRODUCTION	1
SYMBOLS	2
APPROACH	4
EXPERIMENT DESIGN	5
Controlled Failure-Mode Apparatus	5
Range Instrumentation	8
EXPERIMENTAL RESULTS AND DATA ANALYSES	10
CONCLUSIONS	20
APPENDIX A — DETAILED DATA ANALYSES	21
APPENDIX B — PHOTOGRAPHIC TECHNIQUE	26
REFERENCES	28

TABLES

Table		Page
I	TEST VARIABLES FOR CONTROLLED FAILURE-MODE TESTS . . .	7
II	PIEZOELECTRIC TRANSDUCER DATA	11
III	YIELD OF PROPELLANTS IN POUNDS OF TRINITROTOLUENE . . .	13
IV	THE LOX/LH ₂ TESTS	19
V	COMPARISON OF PROPELLANTS	19
A-I	SCALED BLAST PARAMETERS	22

FIGURES

Figure		Page
1	Test fixture	6
2	Test-site instrumentation layout	9
3	Comparison of yield with radius from gage pressure	14
4	Comparison of yield with radius from impulse	14
5	Comparison of yield with radius from time of arrival	15
6	Comparison of normalized yields with a contact area A_c of 36.8 ft^2	16
7	Normalized yields of LOX/LH ₂ tests	16
8	Effect of contact area on yield	17
9	Terminal yield compared with contact area	18
B-1	Geometric corrections of the shock wave	26
B-2	Fireball and shock-wave radii from LOX/LH ₂ tests compared with time	27
B-3	Comparison of photographic data from the three propellant systems with the same A_c	27

SOME LIQUID OXYGEN/LIQUID HYDROGEN EXPLOSIVE EFFECTS IN CONTROLLED FAILURE-MODE TESTS

By Richard W. High
Manned Spacecraft Center

SUMMARY

The explosive yield of liquid oxygen/liquid hydrogen is compared with the yield of nitrogen tetroxide/Aerozine-50 and liquid oxygen/kerosene in controlled failure-mode tests. The comparison suggests that, on the basis of equal interface areas of contact, the potential blast hazard of liquid oxygen/liquid hydrogen is similar to that of the other two systems under some severe failure conditions. This comparison does not consider the effects of the later vapor-phase reactions.

In the tests to determine the effect of the interface area of contact, it is found that the explosive yield of the hydrogen system is proportional to the interface area. The result of this study indicates that it may not be reasonable to use the present hazard criteria for launch vehicles.

INTRODUCTION

The potential explosive hazard of high-energy propellants to be used on launch vehicles must be evaluated to establish safety design and facilities site criteria. When the manned space programs were conceived, these blast hazards¹ were not known for some of the propellant combinations. Failure experience of fueled vehicles is a major source of information that is usable in evaluating the potential explosive hazards of propellants. However, failure experience is essentially nonexistent for two of the three liquid-propellant types used on the launch vehicles. Therefore, a method for evaluating the potential explosive hazards of these systems without failure statistics is needed. Because of time and expense considerations, a controlled comparison technique was developed to compare the propellants of unknown hazard potential to the propellant having failure experience. The technique involved providing controlled failure-mode experiments to test the blast parameters of the various propellants under similar circumstances. Thus, the comparative results from the experiments can be used to estimate the potential blast hazards of the unknown propellants.

¹The blast hazard is a function of the peak overpressure and pulse duration behind the shock front and should not be confused with the thermal hazard presented by the associated fireball.

By using the comparison philosophy, a two-phase experimental program was initiated by the NASA Manned Spacecraft Center to test the blast hazards of nitrogen tetroxide/Aerozine-50² ($N_2O_4/A-50$), liquid oxygen/liquid hydrogen (LOX/LH₂), and liquid oxygen/kerosene (LOX/RP-1). The established failure experience of the latter propellant then can be used as a guide to estimate the potential hazards of the other propellants.

Phase I of this program was in support of the Gemini Program. Propellants $N_2O_4/A-50$ and LOX/RP-1 were tested in phase I in similar test devices. Phase II was in support of the Apollo Program and compares LOX/LH₂ with the two propellants of phase I.

The purpose of this document is threefold: (1) to present the comparison philosophy used, (2) to rank the potential explosive hazards of the three propellants considered under this comparison philosophy, and (3) to discuss the validity and possible limitations of this philosophy. In particular, the comparison between LOX/LH₂ and LOX/RP-1 should assist in reducing some of the uncertainty in the explosive potential criteria of LOX/LH₂ used by NASA for flight vehicles; therefore, this is a primary objective in this document.

The experimental program included parametric evaluations of the shock wave, fireball expansion, temperature, thermal radiation, and fragmentation. The efforts to measure the velocity of some metal fragments and to measure the fireball temperature and radiation were not successful. The data analyses and comparisons presented in this document are concerned primarily with the measurements of shock-wave characteristics, although some fireball size versus time curves (taken from photographic data) are included in the appendix B.

The author wishes to express his gratitude to Mr. R. F. Fletcher for the conception and management of the experimental programs required to obtain the data reported in this document and for his advice and constructive suggestions that permitted preparation of this document. Also, the technical help and comments of Mr. H. A. Zook were a great aid in the completion of this document.

SYMBOLS

A_c	interface area of initial contact between fuel and oxidizer, ft ²
$A_{c(\text{small})}$	contact area of the smallest test size = 25.1 ft ²
a	ambient velocity of sound, ft/msec

²A typical Aerozine-50 blend is a mixture by weight of approximately 48.5 percent unsymmetrical dimethylhydrazine, 51 percent hydrazine, and 0.5 percent water.

\bar{a}	ratio of ambient sound velocity to that at standard conditions
a_0	velocity of sound at standard conditions, ft/msec
I_s	positive phase side-on impulse, psi-msec (Side-on data are measured parallel to the direction of shock-wave propagation and therefore do not include the dynamic pressure from the flowing fluid.)
I'_s	Scaled impulse $I_s \bar{a} / (W/\bar{P})^{1/3} \bar{P}$, psi-msec/lb ^{1/3}
K	constant, equal to $\frac{(\gamma + 1)}{2\gamma P_0}$
P	ambient atmospheric pressure, psia
\bar{P}	ratio of ambient pressure to that at sea level
P_0	atmospheric pressure at sea level, psia
P_s	peak side-on overpressure, psi
P'_s	scaled overpressure P_s / \bar{P} , psi
R	distance from center of explosion, ft
S	area ratio $A_c / A_{c(\text{small})}$
t	time
t'	scaled shock-arrival time $t_m \bar{a} / (W/\bar{P})^{1/3}$, msec/lb ^{1/3}
t_c	calculated shock-wave travel time, msec
t_m	measured shock-wave travel time, msec
U	ambient shock-front velocity, ft/msec
U_0	shock-front velocity at standard conditions, ft/msec
W	equivalent weight of trinitrotoluene, lb
W_t	terminal yield (in terms of equivalent weight of trinitrotoluene, lb)
$W_{t(\text{small})}$	terminal yield of the smallest test size

W_p	propellant weight (weight of fuel plus weight of oxidizer), lb
Z'	scaled distance $\frac{R}{(W/\bar{P})^{1/3}}$, ft/lb ^{1/3}
Z_i	intermediate scaled distances, ft/lb ^{1/3}
γ	ratio of specific heats
'	scaled quantities

APPROACH

To compare the explosive hazards of different propellant combinations without actual launch-vehicle-failure experience, appropriate experimental simulation is required. The events that lead to an explosive reaction between the oxidizer and fuel undoubtedly vary greatly from failure to failure and depend upon the circumstances of each particular failure. However, the purpose of this document is not to consider all the possible variations in explosive yields of a single propellant (oxidizer plus fuel) but, by controlling the mode of failure, to consider a single-failure condition to permit comparison of one propellant with another. Thus, it will be helpful to visualize the following postulated events and consequences in an explosive reaction from a launch-vehicle failure.

1. The propellant tanks rupture, spilling fuel and oxidizer (cause unspecified).
2. The fuel and oxidizer come into contact and mix.
3. The ignition takes place after some finite mixing time.
4. The resulting explosive yield is proportional to the amount of mixed propellant.
5. The amount of mixed propellant is proportional to the mixing time between the tank rupture and the ignition and to the contact area A_c established at the time of rupture. Therefore, explosive yield is proportional to A_c at constant mixing time. This hypothetical consequence had to be tested in the phase I experimental program.

If the previous outline represents a valid picture of the events in a launch-vehicle failure, then another assumption is required to compare the explosive hazards of $N_2O_4/A-50$ and LOX/LH_2 to that of $LOX/RP-1$. Thus, under identical geometrical conditions, it is assumed that the amount of mixing that will take place before ignition for the $N_2O_4/A-50$ and the LOX/LH_2 propellants is not more than that required for the $LOX/RP-1$ propellant. This assumption is developed from the experimental

observations that the ignition energies of $N_2O_4/A-50$ and LOX/LH_2 are not greater than the ignition energy of $LOX/RP-1$ and from the assumption that systems with similar ignition energies have similar delays between tank rupture and explosive reaction. Hence, it is assumed in this document that the average contact area reasonably represents the amount of mixed propellant before ignition and can be used for comparison of the three propellant systems. The author is not presently aware of any experimental data that would unambiguously verify this important assumption. Such data would be very helpful, as will be seen, in solidly establishing the comparison technique used in this document.

The approach used in this document to compare the explosive hazards of LOX/LH_2 to $LOX/RP-1$ can now be outlined. The comparison for $N_2O_4/A-50$ to $LOX/RP-1$ is made in reference 1. First, it is assumed that, after a launch-vehicle failure, LOX/LH_2 will not mix to a greater degree before ignition than will $LOX/RP-1$. Hence, the representative contact area A_c at time of ignition for LOX/LH_2 will not be greater than that for $LOX/RP-1$, for similar failure conditions and geometries. Second, it is shown experimentally that the explosive yield is proportional to the contact area established at the moment of ignition. Third, it is established experimentally that, for a given A_c , the explosive yield of LOX/LH_2 is similar to that of $LOX/RP-1$. It is deduced then that LOX/LH_2 is not likely to result in a greater explosive yield upon launch-vehicle failure than will $LOX/RP-1$, assuming similar geometrical conditions and not considering later vapor-phase reactions. In this approach, the contact area A_c (not the total propellant weight W_p) must be the important parameter in establishing the yield within the limits of the data presented in this document. This concept can be deduced from the phase I data and is necessary for proper interpretation of phase II data because, in these later tests, the design of the test fixture required that the ratio of A_c to W_p be constant.

EXPERIMENT DESIGN

Controlled Failure-Mode Apparatus

The test device for the study of the controlled failure-mode apparatus was designed to provide a controlled interface area A_c for initial mixing of the fuel and the oxidizer. An aluminum pan was used as a container to hold both the fuel and an arrangement of glass dewars filled with the oxidizer. The oxidizer-to-fuel (O/F) ratio was determined principally by the pan volume; the area of contact A_c depended on the mean radius of the dewars, the number of dewars, and the oxidizer depth in the dewars. A sketch of the test device (as used in phase II) is shown in figure 1.

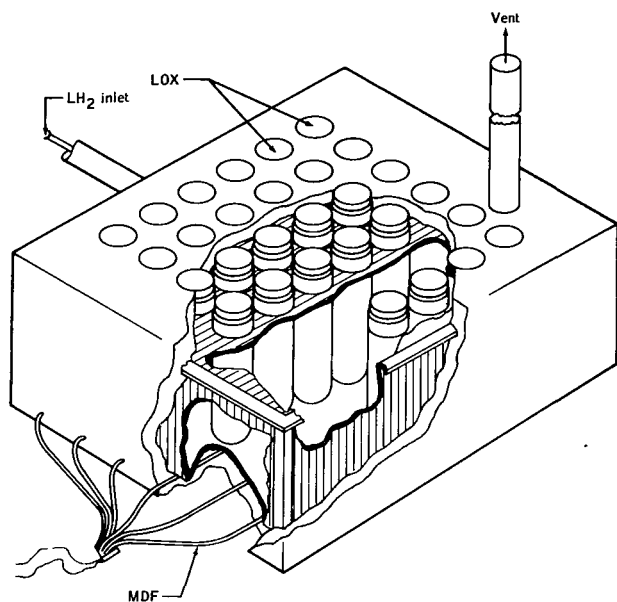


Figure 1. - Test fixture.

In phase I of this program (ref. 1), a propellant weight of 300 pounds was fixed for the tests. The following variables were studied in the first series of 18 tests.

1. Three areas of contact for each propellant
2. Three O/F ratios
3. Two propellant types — $N_2O_4/A-50$ and LOX/RP-1

The dewars in phase I were broken by dropping the entire pan assembly onto a steel plate. This method of shattering the dewars complicated the equipment and produced some off-centered explosions. Another problem in phase I was that the mixed dewar sizes undoubtedly provided a nonuniform mixing environment for comparison purposes. These

problems will be further discussed in the "Experimental Results and Data Analyses" section.

Phase II of the program, which provided for a limited number of tests, did not permit the study of the effects of all variables. The primary objective in the second series of 10 tests was to compare the explosive yield of LOX/LH₂ to LOX/RP-1 and to N₂O₄/A-50. These comparisons were made by using O/F ratios similar to those of fueled vehicles because these were the O/F ratios of greatest interest. The reporting and interpreting of the phase II results are, as previously mentioned, the major purposes of this document.

The second series of 10 tests were performed in the following manner. Two LOX/LH₂ tests were performed at a contact area $A_c = 25.1 \text{ ft}^2$, two were performed at $A_c = 36.8 \text{ ft}^2$, and two were performed at $A_c = 56.2 \text{ ft}^2$. Two LOX/RP-1 tests and two N₂O₄/A-50 tests were performed at the intermediate contact area A_c of 36.8 ft^2 . For experimental reasons, one LOX/LH₂ test and one N₂O₄/A-50 test were unsatisfactory and are not included in this document. To simplify data analyses and interpretation of the contact-area effect, only 1-liter dewars (in a symmetrical arrangement) were used in phase II. Therefore, the fuel and oxidizer volumes were fixed by the dewar volume and the required O/F ratio. To vary the contact area (number of dewars), the total propellant weight also had to vary. This meant that the ratio of contact area to propellant weight A_c/W_p was held constant for all of the LOX/LH₂

tests but varied somewhat for the other propellant systems to control the contact area and the desired O/F ratio. However, the A_c/W_p ratio for LOX/RP-1 was nearly the same as that for LOX/LH₂. A list of the nominal values for each test are provided in table I. Additional discussion of the apparatus will be found in reference 2.

TABLE I. - TEST VARIABLES FOR CONTROLLED FAILURE-MODE TESTS

[Nominal values]

Variable	LOX/LH ₂			LOX/RP-1	N ₂ O ₄ /A-50
	56.2	25.1	36.8		
Contact area A_c , ft ²	56.2	25.1	36.8	36.8	36.8
Propellant weight W_p , lb	225	100	150	171	230
Oxidizer/fuel weight ratio	5:1	5:1	5:1	2.5:1	2:1
$\frac{\text{Contact area}}{\text{Total weight}}$ A_c/W_p	0.25	0.25	0.25	0.22	0.16

To conduct the tests, the dewars were filled with oxidizer to the proper depths, and stoppers were placed on the tops of the dewars to reduce vaporization. The fuel then was remotely added to the space in the pan surrounding the dewars, by the use of controls in the control building. The glass dewars in the phase II test were shattered by detonating 20-grain/foot mild detonating fuse (MDF) under the pan bottom (fig. 1). The pan bottom was designed to resist perforation during the detonation of the MDF while the shock was transmitted through the bottom to completely shatter the glass dewars. Shattering the glass dewars allowed the fuel and oxidizer to mix. The effectiveness of this concept for dewar shattering was tested thoroughly before the phase II tests were begun. The test explosion was initiated spontaneously from an unknown source — perhaps the shock from dewar implosion. See reference 2 for other possible sources. In addition, for the LOX/LH₂ series, there were several other requirements. Two of these requirements are insulation of the test pan containing liquid hydrogen and use of a special instrument for sensing the liquid level.

As a reference for the tests and calibration of the instruments, a series of 10-, 25-, 50-, and 100-pound trinitrotoluene (TNT) charges were detonated and were compared with TNT data from the Ballistics Research Laboratory.

Range Instrumentation

Instrumentation for these tests included piezoelectric and mechanical gages to measure shock-wave characteristics, cameras to measure the fireball and shock-wave expansion rates, and heat and temperature sensing instruments to measure fireball temperatures and heat flux. A diagram of the test site and location of the instruments is presented in figure 2. Piezoelectric pressure transducers were stationed at 25, 40, 60, and 80 feet from the test center to measure the pressure-time histories of the shock wave. The signals from these gages were fed through calibration units and low-impedance amplifiers to a 14-channel magnetic tape recorder. To obtain permanent records needed for data reduction, these signals were played back from the tape recorder to a recording oscillograph. Three rows of these gages were provided at angular displacements of 120° to measure the concentricity of the shock wave. Peak overpressure, positive phase impulse, and arrival time of a shock wave were determined from these pressure-time measurements.

Mechanical self-recording gages were positioned along two of the pressure gage lines at 40-, 60-, 80-, and 98-foot locations. These gages — supplied and operated by the Ballistic Research Laboratory — were provided to give duplicate measurements of the shock-wave parameters. The deflections of the scribed records from these gages are compared by microscopic examination with deflections from calibration tests to determine the peak overpressures and impulses.

Photographic instrumentation was used extensively for this program to gather information on the expansion of the fireball and the shock wave. Most of the cameras and much of the assistance in proper operation of this equipment was supplied by the Photographic Technology Laboratory at the Manned Spacecraft Center, Houston, Texas.

The test site contained two camera locations that were located at angular displacements of 68° from each other. From these locations, two cameras with infrared (IR) film and two cameras with color film recorded the motion of the fireball and the shock wave. Reference poles in the field of view and timing marks on the film were used for event-size measurement and timing. The IR cameras operated at approximately 5500 frames/second to provide an accurate recording of the initial fireball motion. The full duration of the fireball was recorded by a camera that operated at 400 frames/second and by another camera that operated at 1000 frames/second.

Information about fireball temperature gradient, radiant heat flux, and total radiation was desired from this program. To measure these parameters quantitatively, thermal instrumentation was required with faster response times than those from instruments normally available. A sensor development program was required to supply sensors which had satisfactory resistance to the pressure and temperature environment and which had the fast-response capability. Part of the development program was conducted by the Instrumentation and Electronic System Division at the Manned Spacecraft Center. They developed a system which contained a thermocouple, a heat-flux gage, and a radiometer. These instruments were stationed at 10-, 15-, 25-, and 35-foot radii from the fireball center. Little significant data were obtained from this program. The development and data obtained are contained in reference 3. A second program was conducted by Midwest Research Institute to develop a preheated thermocouple system to measure the fireball temperature gradient. Experimental instruments were stationed at 10, 15, 20, and 25 feet from the test center. A few

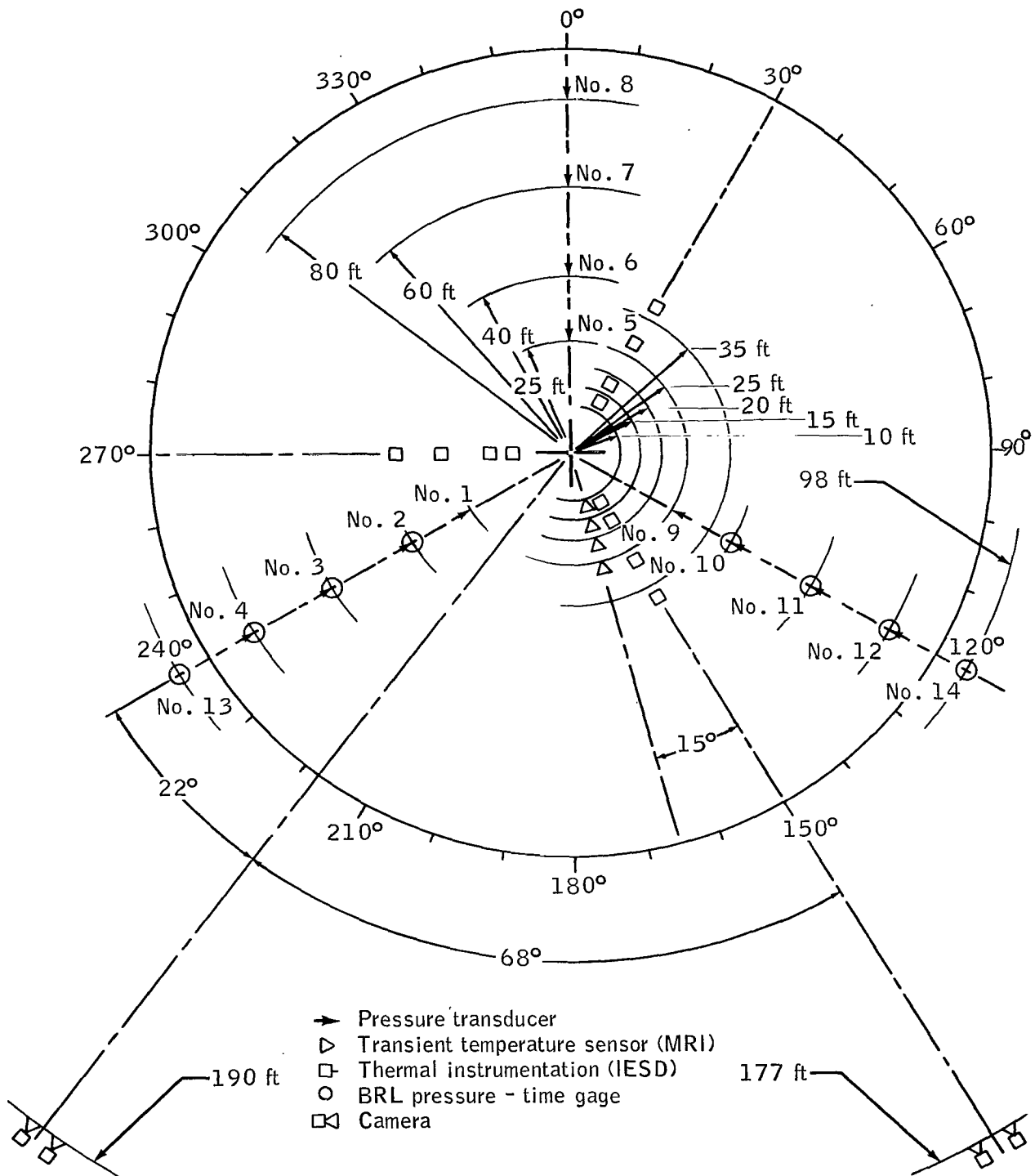


Figure 2. - Test-site instrumentation layout.

temperature readings were obtained to provide confidence in the feasibility of the system; however, there were not enough data to describe the temperature gradient of the fireball. This program and the data from the tests are presented in reference 4.

Several devices were tested in an attempt to measure the velocities of fragments leaving the detonation. These devices included fragments traveling on wires, metal spheres with wires attached that would break a series of electrical probes, and measurement of free-flying fragments from film records. This program is described in reference 2.

EXPERIMENTAL RESULTS AND DATA ANALYSES

As stated previously, one of the purposes of this document is to rank the explosive hazards of the three propellants considered under the comparison philosophy presented in the "Approach" section. The explosive hazards of the propellants are ranked by comparing the equivalent TNT yields of these propellants. The propellant yields are expressed in terms of pounds of TNT. Because the energy of detonation of TNT is approximately 1 kilogram calorie/gram (1.018 kg cal/g is given in ref. 5), the propellant yields in pounds of TNT can easily be converted to energy terms, if desired. The TNT yield is used in this document because it is commonly understood in the field of explosions and hazard evaluations.

The equivalent yields are computed from the overpressure measurements or from the side-on impulse³ measurements at known distances from the explosion. The yields can also be independently computed from time-of-flight data of the blast pulse. The equations necessary for carrying out these computations are presented in appendix A. For the phase II tests, the overpressure, side-on impulse, and time-of-flight data from the piezoelectric transducers are presented in table II. The yields computed from these data are presented in table III and in figures 3 to 5. The data analyses presented in this document are based on the piezoelectric transducer results. Shock-wave parametric data were also obtained from mechanical pressure-time gages by the Ballistic Research Laboratory (ref. 2). Because the data from the mechanical gages were not as complete as the electronic data and because the scatter of data was greater, a separate analysis for the gages was not made. However, the overpressure data obtained from the mechanical gages agree reasonably well with the data obtained from the piezoelectric transducers and lend support to the reliability of the latter data. Photographic data on the velocity of travel of the shock wave and fireball were also obtained. The photographic shock-wave data also support the piezoelectric results. The photographic technique is described in more detail in appendix B.

³The side-on impulse is determined by integrating the area of the positive phase region under the pressure versus time curve of the blast wave as sensed by a pressure transducer properly placed with the sensitive face parallel to the direction of travel of the pulse.

TABLE II. - PIEZOELECTRIC TRANSDUCER DATA

[From ref. 2]

Test	A _c , ft ²	Ambient air temperature, °F	Ambient atmospheric pressure P, psia	Gage data			Shock-wave travel-time data		
				Distance, ft	Peak overpressure	Positive impulse	Gage distance, ft		Time t _m , msec (a)
					P _s , psi (a)	I _s , psi-msec (a)	From	To	
LOX/LH ₂	25.1	92	14.686	25	23.7	58.0	--	--	--
				40	8.7	36.3	25	40	9.81
				60	5.0	22.9	40	60	14.80
				80	3.0	13.4	60	80	15.81
LOX/LH ₂	25.1	82	14.096	25	19.9	55.1	--	--	--
				40	8.9	34.9	25	40	10.12
				60	4.7	20.8	40	60	14.93
				80	3.0	16.5	60	80	15.73
LOX/LH ₂	56.2	81	14.096	25	35.7	87.4	--	--	--
				40	15.4	57.3	25	40	8.45
				60	7.2	35.3	40	60	13.66
				80	5.2	24.3	60	80	14.76
LOX/LH ₂	56.2	80	14.145	25	28.3	75.1	--	--	--
				40	13.2	56.0	25	40	8.90
				60	6.8	38.8	40	60	13.86
				80	4.3	24.0	60	80	15.20

^a Average values from three separate gages located 120° apart at each radial position.

TABLE II. - PIEZOELECTRIC TRANSDUCER DATA - Concluded

[From ref. 2]

Test	A_c , ft ²	Ambient air temperature, °F	Ambient atmospheric pressure P, psia	Gage data			Shock-wave travel-time data		
				Distance, ft	Peak overpressure P_s , psi (a)	Positive impulse I_s , psi-msec (a)	Gage distance, ft		Time t_m , msec (a)
							From	To	
LOX/LH ₂	36.8	86	14.096	25	22.7	62.8	--	--	--
				40	9.7	41.1	25	40	9.52
				60	5.0	27.5	40	60	14.66
				80	3.7	19.6	60	80	15.48
LOX/RP-1	36.8	59	14.047	25	25.9	49.0	--	--	--
				40	11.5	38.9	25	40	9.08
				60	5.9	27.5	40	60	14.21
				80	3.5	24.0	60	80	15.52
LOX/RP-1	36.8	81	14.096	25	31.5	68.0	--	--	--
				40	12.4	39.6	25	40	8.00
				60	7.4	35.4	40	60	13.71
				80	4.2	29.6	60	80	15.12
N ₂ O ₄ /A-50	36.8	88	14.145	25	24.6	59.0	--	--	--
				40	11.1	37.9	25	40	9.26
				60	5.4	27.2	40	60	14.37
				80	3.6	21.2	60	80	15.35

^a Average values from three separate gages located 120° apart at each radial position.

TABLE III. - YIELD OF PROPELLANTS IN POUNDS OF TRINITROTOLUENE

Radius, ft	LOX/LH ₂ at A _c equal to -					LOX/RP-1 at A _c equal to -		N ₂ O ₄ /A-50 at A _c equal to -	
	25.1 ft ²	25.1 ft ²	56.2 ft ²	56.2 ft ²	36.8 ft ²	36.8 ft ²	36.8 ft ²	36.8 ft ²	
Yield (pressure)									
25	47.9	46.5	102.6	75.2	55.7	66.6	86.8	62.2	
40	55.0	57.7	132.5	105.8	66.4	86.5	96.6	81.4	
60	71.7	68.0	140.6	126.7	74.1	101.2	116.4	85.6	
80	63.3	67.5	161.1	131.0	91.7	91.9	129.5	98.2	
Yield (impulse)									
25	56.5	68.4	161.9	127.3	96.9	73.7	108.7	87.9	
40	78.1	73.9	162.2	155.2	96.1	85.1	100.7	85.0	
60	67.1	58.5	133.8	154.7	90.3	88.1	135.3	89.9	
80	44.5	62.4	113.0	111.2	95.3	90.2	128.4	92.2	
Yield (time of arrival)									
25 to 40	50.3	48.6	120.6	93.8	61.1	93.2	134.9	72.8	
40 to 60	59.7	57.5	140.7	125.5	68.1	120.4	136.5	85.8	
60 to 80	66.3	71.0	188.6	150.2	91.8	130.7	140.7	103.8	
Terminal yield, W _t									
	53.9	65.0	137.1	121.1	93.5	91.1	129.0	95.2	

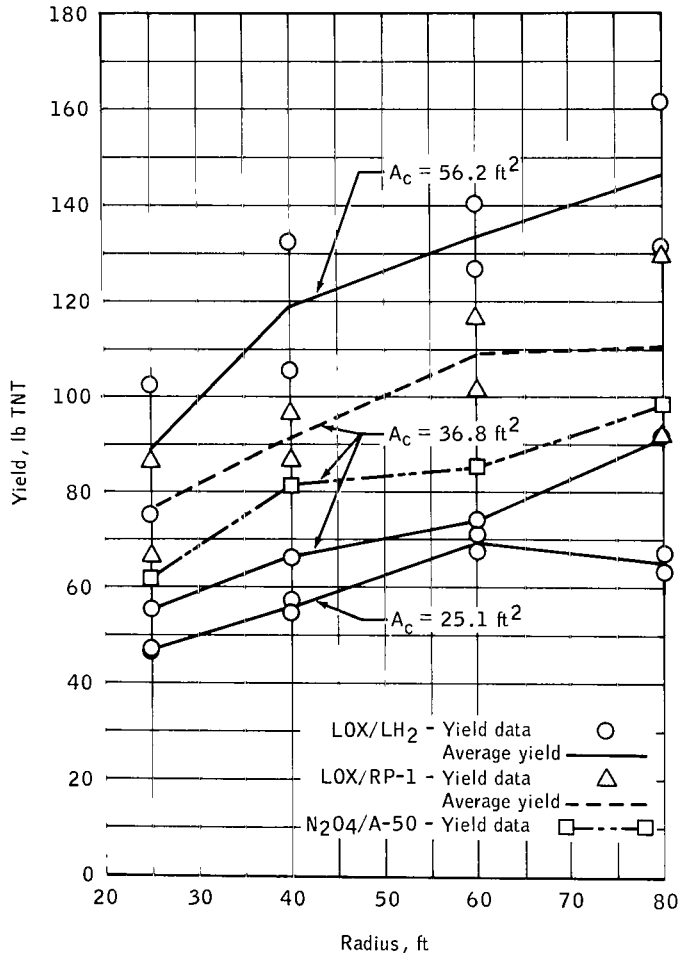


Figure 3. - Comparison of yield with radius from gage pressure.

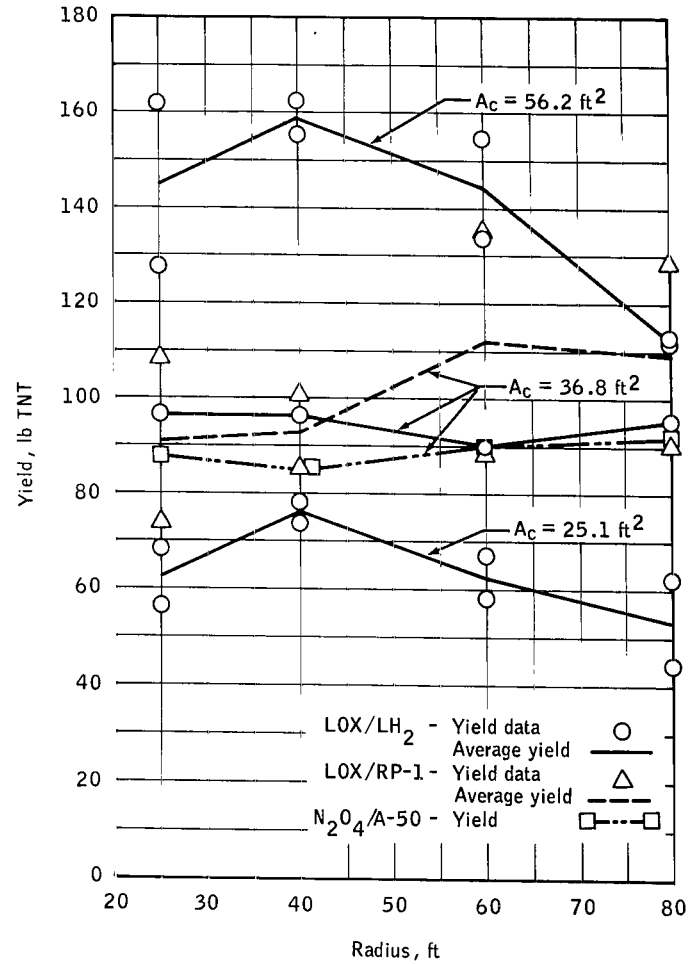


Figure 4. - Comparison of yield with radius from impulse.

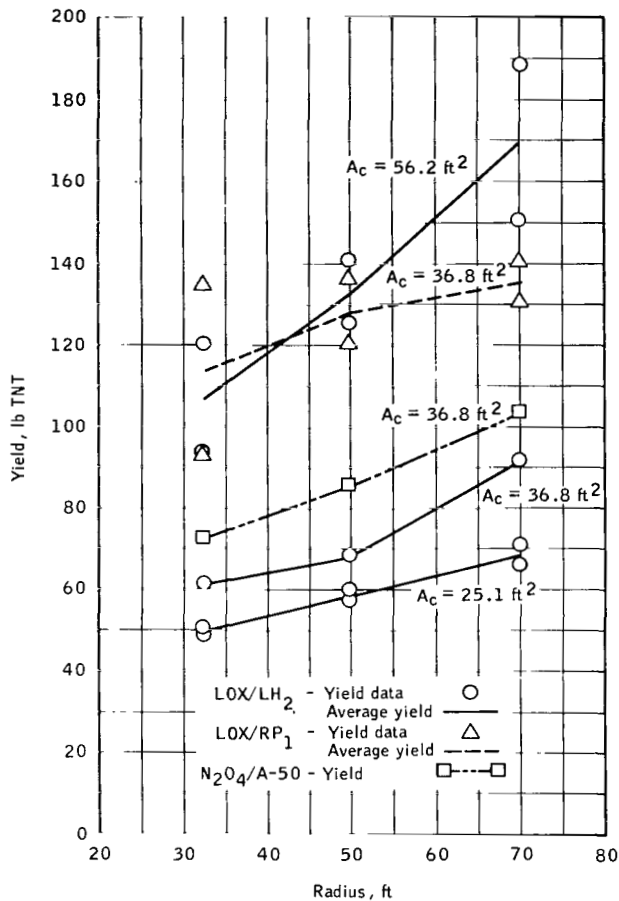


Figure 5. - Comparison of yield with radius from time of arrival.

shown in figure 7. The trends are roughly independent of test size (fig. 7).

The difference in blast-wave shape between a propellant explosion and a high explosive detonation is probably the result of the nonhomogeneous nature of the propellant mixture which would produce a series of small explosions in the mixed portion of the propellant instead of a single detonation. Because the trailing shock fronts (produced after the leading shock front) will be traveling in preheated air, the velocities of the trailing shock fronts will be higher than the velocity of the leading shock front in ambient air. Therefore, the trailing shock fronts will catch up to and reinforce the leading shock front. Variations in both the overpressure and the impulse measurements are expected to be introduced by debris, shock-reflection differences, and so forth.

Propellant explosions differ in significant ways from TNT explosions. For example, propellant explosions characteristically exhibit a blast wave having a long duration with a low-pressure shock front at the nearest gage position. The shape of the blast wave changes with distance when compared to a high explosive detonation until, at large distances, a characteristic high explosive shock wave is produced. The change in blast-wave shape produces an increase in yield with distance from overpressure and time-of-flight measurements, but the change generally produces a decrease in yield with distance from impulse measurements when using the data from TNT detonations as a basis for the yield computations. These phenomena can be examined in table III and in figures 3 to 5 for the phase II tests. In figure 6, the data from the three propellants tested at a single contact area have been normalized by dividing the yield at each radial distance by the average yield. Therefore, these normalized values have a value of unity at an approximate intermediate distance and can be compared to TNT with a constant normalized value of unity. Each of the propellants shows a similar trend with distance. The LOX/LH₂ results (after

they have been normalized in a manner similar to that previously discussed) are

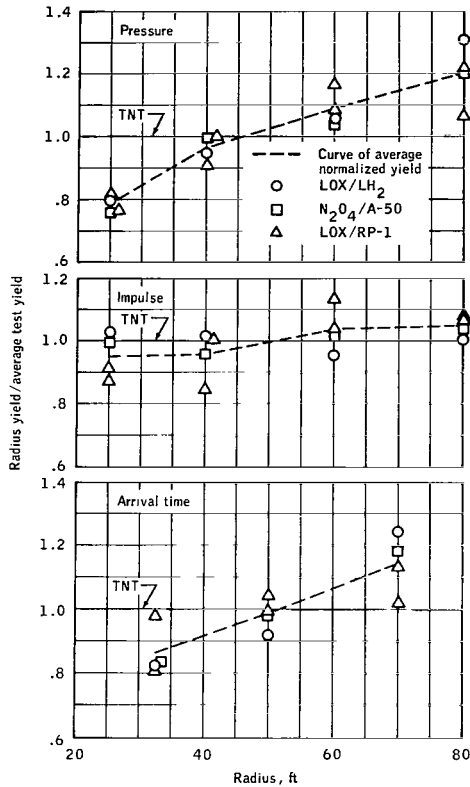


Figure 6. - Comparison of normalized yields with a contact area A_c of 36.8 ft^2 .

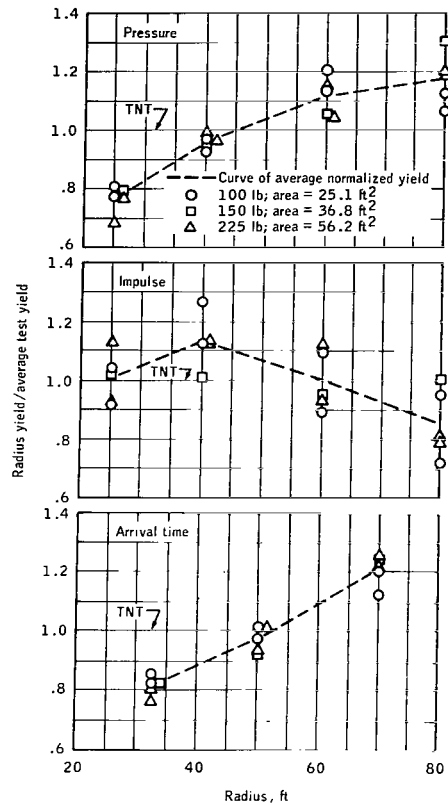


Figure 7. - Normalized yields of LOX/LH₂ tests.

The terminal yield⁴ seems to be the most consistent and meaningful measure of the explosive effect of the various propellants and is therefore the best measure to use for comparison purposes. The terminal yields obtained from the 18 $\text{N}_2\text{O}_4/\text{A-50}$ and LOX/RP-1 tests performed in phase I are shown in figure 8. Each of these tests had a total propellant weight of 300 pounds. The individual data points in figure 8 are represented by symbols; the straight lines are fit to the data by the method of least squares. The terminal yield depends heavily upon the contact area A_c involved. Also, large changes in the O/F ratio do not affect the terminal yield by correspondingly large amounts (fig. 8), as seen by observing the data fit lines. Thus, these data (at constant propellant weight) suggest a rather complicated relationship between

⁴Terminal yield is the equivalent TNT explosive yield in a region where explosive yield becomes independent of distance from the explosion or of the shock-wave parameter used in the calculations. For the purposes of this document, the previously mentioned conditions were considered to be satisfied by averaging the impulse and the pressure yield at the gage position farthest from the center of the explosion.

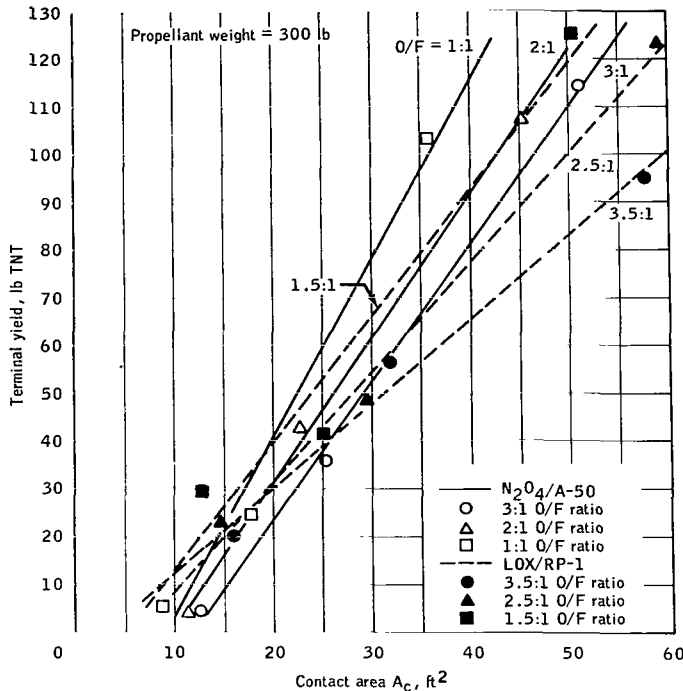


Figure 8. - Effect of contact area on yield.

comparisons more meaningful. The total participation of the propellants in the explosive yields of the phase I tests varied from "zero" to less than 25 percent of the theoretical maximum⁵. With these small fractions of the ultimate yield plus the strong dependence of yield to A_c (fig. 8) at a constant propellant weight, it seems reasonable to conclude that the propellant weight is not the important parameter in these tests. Data are not available to conclusively prove this relationship at other constant-weight conditions; however, data from phases I and II could be compared to observe the effect of a constant propellant weight and a variable propellant weight. Actually, from the more uniform experimental conditions of phase II, more effective participation of the propellant resulted in higher yields with less total propellant at similar contact areas. This does not mean that such a trend would exist with this test device but rather that the phase II tests were more efficient and that the propellant weight is not the important parameter. Of course, variations in propellant weight considerably beyond the limitations of this test program would be expected to have a significant effect on the yield. Thus, with the qualifications mentioned previously, the experiments in phase I demonstrate that the

⁵The ultimate or maximum yields for propellants in this document are approximately 1.6 to 1.7 pounds of TNT/lb of propellant for N₂O₄/A-50 and LOX/RP-1 at 2:1 and 2.5:1 O/F ratios, respectively. The LOX/LH₂ maximum yield is above 2 pounds of TNT/lb of propellant at 5:1 O/F ratio.

parameters, much of which is the result of the geometry of the phase I test configuration which required mixed numbers of dewars and sizes to control both the O/F ratio and the contact area A_c .

The effects of O/F ratio are expected to be the greatest near the optimum mixture; therefore, the data in figure 8 probably display the largest effect of this parameter. The yields for N₂O₄/A-50 and LOX/RP-1 at optimum conditions (intermediate O/F ratios) display similar results (fig. 8).

The most meaningful comparisons of A_c are made when the O/F ratio is fixed, thus reducing the changing geometry effect. Also, the use of only one dewar size in a symmetrical arrangement in the phase II tests should greatly reduce the geometry factors, thus making the com-

terminal yield of exploding propellants is approximately proportional to the contact area between the fuel and oxidizer. Additional work done in phase II with the LOX/LH₂ propellant tends to verify the contact-area/terminal-yield relationship, as shown in table IV and figure 9. Because of more uniform experimental conditions used in the

phase II work, the consistency of the data was improved. Of course, as A_c/W_p

was held constant and the O/F ratio held at optimum, these phase II data do not show that terminal yields have little dependence on W_p . But, if this low dependence of

W_p is assumed to be established from the data in figure 8 and from the low participation in the explosive reaction, then yield as a simple linear function of A_c is the important relationship for these tests.

In table V, the terminal yields of the three propellants are compared at a single contact area $A_c = 36.8 \text{ ft}^2$. The O/F ratios

used were optimum values for the launch vehicle in each case. It is seen that the terminal-yield values thus compared are very similar, with the LOX/LH₂ value be-

ing the smallest. Hence, according to the experimental analysis and the assumed relationship between parameters presented in this document, LOX/LH₂ does not rep-

resent a greater blast hazard than does LOX/RP-1 or N₂O₄/A-50 under identical missile failure.

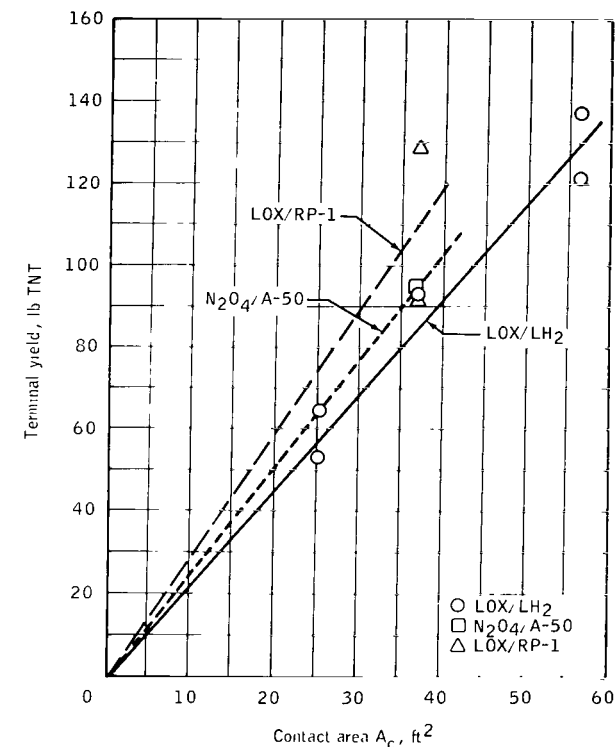


Figure 9. - Terminal yield compared with contact area.

The previous analysis is only as valid as the exactness of the experimental work and the reasonableness of the assumptions. In addition, it should be mentioned that the geometrical factors for launch vehicles actually using LOX/LH₂ are quite different from the geometrical factors for launch vehicles using LOX/RP-1 or N₂O₄/A-50.

Therefore, in applying these results to the launch-vehicle explosive hazards, these geometrical factors must be strongly considered, as well as launch-vehicle size and propellant combination.

TABLE IV. - THE LOX/LH₂ TESTS

A_c , ft ²	Area ratio S, $A_c/A_{c(\text{small})}$	Average terminal yield ^a W_t , lb TNT	Normalized yield $W_t/W_{t(\text{small})}$
25.1	1	59.4	1
36.8	1.47	93.5	1.57
56.2	2.24	129.1	2.17

^a Average terminal yield determined by averaging the yield results of the pressure techniques and the impulse techniques in table III for $R = 80$ ft.

TABLE V. - COMPARISON OF PROPELLANTS

Propellant	A_c , ft ²	Total weight W_p , lb	Weight ratio, W_p (propellant) W_p (LOX/LH ₂)	Average terminal yield, lb TNT
LOX/LH ₂	36.8	150	1	93.5
LOX/RP-1	36.8	171	1.14	110.0
N ₂ O ₄ /A-50	36.8	230	1.53	95.2

CONCLUSIONS

The test device provides a means of controlling the interface area of contact between the fuel and oxidizer. By controlling the interface area, the very short ignition delays permit controlled amounts of propellants to mix prior to ignition, thereby providing a means for comparing the explosive potential of various propellant systems. It should be emphasized that these very short ignition delay times did not allow study of any later gaseous phase reactions between vaporized hydrogen and either vaporized oxygen or ambient air. These later reactions could produce significant explosive yields. For the tests reported in this document, the yields were found to be proportional (within experimental uncertainty) to the contact area between the fuel and oxidizer. This indicates that fairly consistent mixing characteristics and ignition delays were obtained.

By using the blast wave of trinitrotoluene as a standard for yield computations, the yield of liquid propellant explosions from overpressure measurements increases with distance from the center of the explosion; whereas, the yield from impulse often decreases with distance. The terminal yield, determined by averaging the values obtained by both methods of measurement and taken at the farthest distance from the explosion, appears to give the most consistent means for comparing propellant explosions with trinitrotoluene detonations.

The yield produced by the LOX/LH₂ propellant system (after short ignition delay times) is similar to the yields produced by the N₂O₄/A-50 and the LOX/RP-1 propellant systems which have the same contact area. If the ignition delays in LOX/LH₂ launch-vehicle failures are not generally greater than the ignition delays in LOX/RP-1 launch-vehicle failures, then the LOX/LH₂ system should not pose a greater explosive hazard under severe failure conditions than would a LOX/RP-1 system. This assumes that geometrical factors and the causes of failure are similar. The present practice of using a much larger yield criteria for LOX/LH₂ than for LOX/RP-1 probably overrates LOX/LH₂ relative to LOX/RP-1 for reasonable modes of launch-vehicle failure.

Finally, it is felt that additional study could be made of the ignition delay problem and of geometric factors in launch-vehicle failures before the data presented in this document can be used safely to predict LOX/LH₂ launch-vehicle explosive hazards by comparing them to previous LOX/RP-1 failures.

Manned Spacecraft Center
National Aeronautics and Space Administration
Houston, Texas, June 11, 1969
918-50-18-22-72

APPENDIX A

DETAILED DATA ANALYSES

The explosive yield data presented in the figures of this document and in table III were prepared by comparing measured overpressure and impulse per unit area with like values of overpressure and positive phase impulse from TNT (ref. 6). The polynomial relating the scaled peak side-on overpressure P'_s to the scaled distance Z' for TNT was taken from reference 7. The polynomial is derived by a least-squares method of fitting the natural logarithms of 273 TNT data points. Thus

$$\begin{aligned} \log_e P'_s = & 7.0452041 - 1.6277561 \log_e Z' \\ & - 0.27399088 (\log_e Z')^2 - 0.065973136 (\log_e Z')^3 \\ & + 0.0065412563 (\log_e Z')^4 + 0.048236359 (\log_e Z')^5 \\ & - 0.020072553 (\log_e Z')^6 + 0.0030190449 (\log_e Z')^7 \\ & - 0.00015984026 (\log_e Z')^8 \end{aligned} \quad (1)$$

for $0.5 \leq Z' \leq 70$.

The original data used to develop this equation were adjusted to standard sea-level conditions to give the scaled overpressure. For test data at other than standard conditions, the scaled values were computed to compare with the TNT data at standard conditions. The scaled blast parameters based on Sach's scaling laws (ref. 8) are shown in table A-I.

A polynomial regression analysis was applied to impulse data (ref. 9) to produce a relationship between scaled impulse and scaled distance. The following equation from the regression analysis was used to analyze the impulse test data.

$$\begin{aligned} \log_e (I'_s) = & 4.2292597 - 1.02447563 \log_e Z' \\ & + 0.07900453806 (\log_e Z')^2 - 0.01882975489 (\log_e Z')^3 \\ & + 0.001180597037 (\log_e Z')^4 \end{aligned} \quad (2)$$

for $2.7 \leq Z' \leq 450$.

TABLE A-I. - SCALED BLAST PARAMETERS^a

Symbol	Scaled blast parameter	Description
P'_s	P_s/\bar{P}	Scaled overpressure, psi
I'_s	$\frac{I_s \bar{a}}{(W/\bar{P})^{1/3} \bar{P}}$	Scaled impulse, psi msec/lb ^{1/3}
Z'	$\frac{R}{(W/\bar{P})^{1/3}}$	Scaled distance, ft/lb ^{1/3}
t'	$\frac{t_m \bar{a}}{(W/\bar{P})^{1/3}}$	Scaled shock-arrival time, msec/lb ^{1/3}

^aRatio of ambient pressure to that at sea level $\bar{P} = P/14.7$. Ratio of ambient sound velocity to that at standard conditions $\bar{a} = a/1.139$.

The relationship between peak overpressure and shock-wave velocity is given by the Rankine-Hugoniot equation. By assuming that the gas is described adequately by the ideal gas law, the following equation can be derived.

$$\frac{P_s}{P} = \frac{2\gamma}{(\gamma + 1)} \left(\frac{U^2}{a^2} - 1 \right) \quad (3)$$

The shock-wave velocities can be determined by measuring the arrival time at the piezoelectric gages and by measuring the distance between the gages. Accurate determination of "zero" time was not possible, so the velocities were determined only for the intervals between the gages. By dividing the difference in arrival times by the distance between gages, an average velocity was calculated. The use of an average velocity is not strictly correct because the shock decay is an exponential function rather than a linear function of the distance traveled. This simplification results in calculated pressures which are higher than the actual pressures if the pressures are compared at the average distance.

An integrated function of the Rankine-Hugoniot equation was used for analysis of the arrival-time data for this document; the pressure from the average velocity was used to confirm the analysis. The computational scheme was developed at the Marshall

Space Flight Center and was completed and programed at the Manned Spacecraft Center for use in analyzing these data. In this program, equation (3) is rearranged to give

$$\frac{a}{U} = \left[\frac{P_s}{P} \frac{\gamma + 1}{2\gamma} + 1 \right]^{-1/2} \quad (4)$$

where the velocity of the shock front U is

$$U = \frac{dR}{dt} \quad (5)$$

In scaled quantities, equation (5) becomes

$$U_0 = \frac{dZ'}{dt'} \quad (6)$$

where U_0 is the velocity at standard conditions. Equation (7) was obtained by multiplying equation (6) by a_0 and then by rearranging and integrating the equation.

$$a_0 t' = \int_{t'_1}^{t'_2} a_0 dt' = \int_{Z'_1}^{Z'_2} \frac{a_0}{U_0} dZ' \quad (7)$$

where a_0 is the velocity of sound at standard conditions.

Equation (8) is obtained by substituting the scaled values for equation (4) into equation (7).

$$\begin{aligned}
 a_0 t' &= \int_{Z'_1}^{Z'_2} \frac{a_0}{\bar{U}_0} dZ' = \int_{Z'_1}^{Z'_2} \left[\frac{(\gamma + 1)}{2\gamma} \frac{P'_s}{P_0} + 1 \right]^{-1/2} dZ' \\
 &= \int_{Z'_1}^{Z'_2} (KP'_s + 1)^{-1/2} dZ'
 \end{aligned} \tag{8}$$

where $K = \frac{(\gamma + 1)}{2\gamma P_0}$.

Because $\log_e P'_s = f(Z')$ from equation (1), equation (8) can also be expressed as

$$a_0 t' = \int_{Z'_1}^{Z'_2} \left[Ke^{f(Z')} + 1 \right]^{-1/2} dZ' \tag{9}$$

From equation (8), the equation for the calculated travel time between gages including the quantities scaled for standard conditions is as follows.

$$t_c = \frac{W^{1/3}}{a(\bar{P})^{1/3}} \int_{Z'_1}^{Z'_2} (KP'_s + 1)^{-1/2} dZ' \tag{10}$$

where the limits Z'_1 and Z'_2 must also be standardized.

The computer program computes a table of values for Z' compared with

$$\sum_{i=1}^n \int_{Z'_{(i-1)}}^{Z'_i} \frac{dZ'}{\sqrt{KP'_s + 1}}$$

where $Z'_0 = 0.5$ and $Z'_n = Z'$ before calculating the yield from data points. Then, a value for a shock-arrival time and the associated distances and the meteorological data are selected. From these data, the yield (in pounds TNT) is computed by (1) starting with an estimate of the yield, (2) computing the values for Z'_1 and Z'_2 from this estimate, (3) locating the values for the integral at the computed Z' values from the table (interpolating between tabulated values if required), and (4) calculating a travel time by using equation (10). This calculated travel time is then compared with the measured value, and an adjustment is made to the TNT yield based on this comparison. This process is repeated until a yield is determined that makes the calculated and measured shock-travel times agree. The values of these yields agreed reasonably well with those from the gage overpressure measurements.

Measurement of arrival time, overpressure, and side-on impulse provides three separate means for measuring the energy of the blast wave. These methods complement one another to provide confidence in the results. Agreement between yield from shock-arrival time and from overpressure provides confidence in the overpressure results because the uncertainties in the measurements of the data are different for each method. The main uncertainties in direct overpressure measurement are the variations in recording pulse amplitude and in gage calibrations; whereas, the arrival time method is subject to uncertainties in measurement of time, sonic velocity, and distance between gages. The overpressure is a measure of the energy in the shock front. The impulse, however, reflects the total energy of the blast wave and, therefore, may be a better method for measuring the energy released in explosions of liquid propellants. The impulse is more susceptible to deviations from reflections, debris, and so forth in its path, thus resulting in more data scatter than that from peak-pressure measurements. Therefore, it is most useful as a supplement to the overpressure data.

APPENDIX B

PHOTOGRAPHIC TECHNIQUE

Most of the visible shock-wave data from the camera films were obtained by observing the boundary of the illuminated circle on the ground. This illuminated area is produced when light from the fireball is reflected by the discontinuity in the air density at the shock front. The leading edge of the shock wave could be observed shortly after the shock wave separated from the fireball; the radius of the shock wave was measured until the pressure dropped to a point at which the density discontinuity at the pressure front was insufficient to produce a visible image on the film. The expanding shock-wave radius must be measured relative to a reference point in the field of view of the camera. Geometric corrections were achieved by projecting the tangent to the expanding shock wave from the camera onto a known radius as seen in figure B-1.

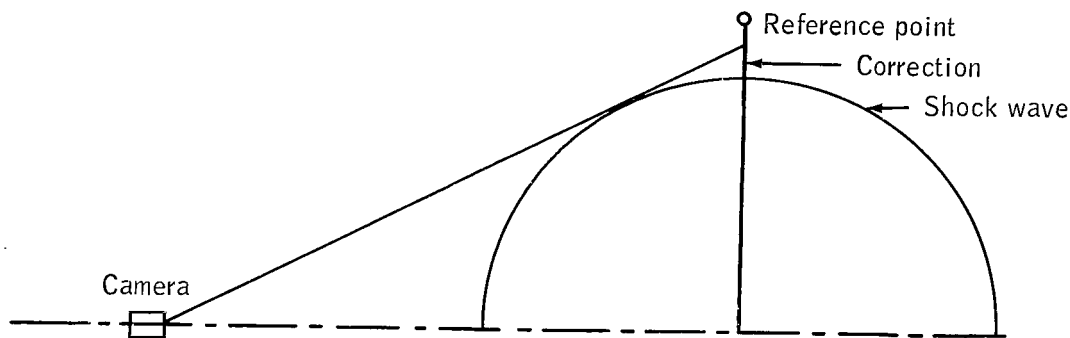


Figure B-1. - Geometric corrections of the shock wave.

Also, a correction was made to the time of each frame so that the expansion curves would extrapolate to "zero" time because this value was not accurately measured in the experiments. With these corrections, the individual curves for each test displayed consistent expansion rates. The shock-wave curves presented in figures B-2 and B-3 were prepared by subjecting the individual radius versus time measurements to a polynomial regression analysis. Some curve smoothing was applied to the curves (figs. B-2 and B-3) beyond 15 milliseconds to compensate for scatter in the composite data. The radius compared with time data for the LOX/LH₂ tests are plotted in figure B-2. From these curves, it is seen that by increasing the area of contact A_c , the slope of the shock-wave expansion curve increases. The comparison of the three propellants with a constant area of contact A_c is shown in figure B-3. The shock-wave curves for three of the tests were similar. This is consistent with the TNT yield calculations for these tests. One LOX/RP-1 shock-wave curve exhibits a greater slope than that of the other shock waves on figure B-3. This same result is also noted in the yield data in which one of these tests produced a higher yield than the other tests presented on this curve.

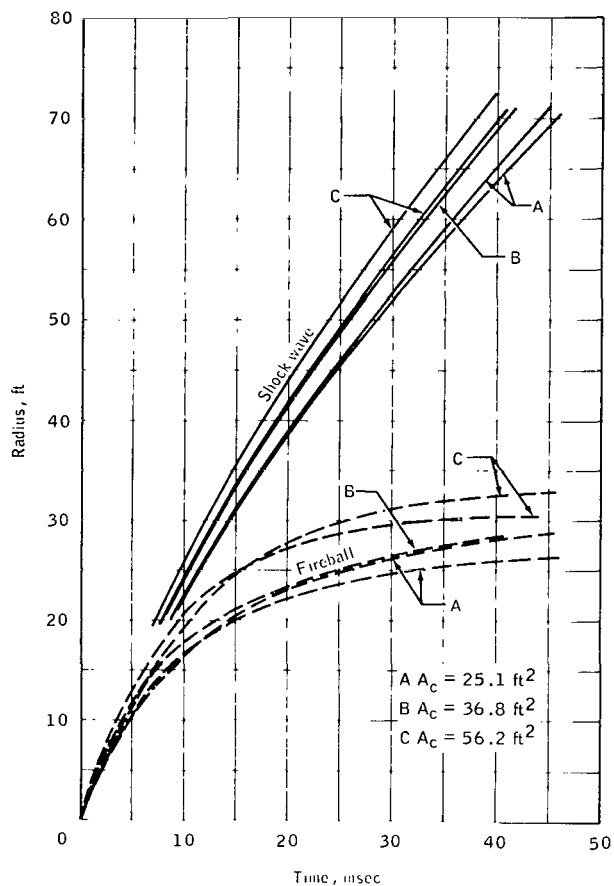


Figure B-2. - Fireball and shock-wave radii from LOX/LH₂ tests compared with time.

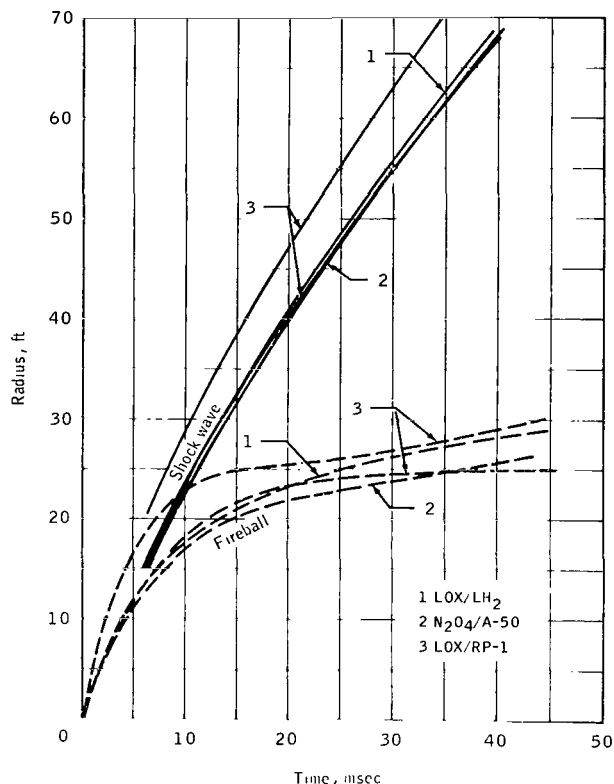


Figure B-3. - Comparison of photographic data from the three propellant systems with the same A_c .

The film data are not sufficiently accurate to permit calculations of yields to be made with the accuracy of those made from the electronic data. The primary objectives in presenting these photographic data are to illustrate that film data can provide an independent means of estimating the effect of changing contact area on explosive potential and to show that some generalizations can be made from optical data which agree with the data from the piezoelectric transducers.

Measurements of the radii of the external surfaces of the fireballs from the photographic records were treated in a manner similar to that of the shock front discussed previously. These curves will also be found in figures B-2 and B-3. The radii of the later phases of the fireball should be principally a function of the amount of propellant. However, because of data scatter, this trend is not obvious on these figures.

REFERENCES

1. Pesante, R. E., et al.: Blast and Fireball Comparison of Cryogenic and Hypergolic Propellants. Aerojet-General Corp. Rept. 0822-01 (01)FP, Contract NAS 9-2055, June 1964.
2. Pesante, R. E.; and Nishibayashi, M.: Evaluation of the Blast Parameters and Fireball Characteristics of Liquid Oxygen/Liquid Hydrogen Propellant. Final report, Aerojet-General Corp. Rept. 0954-01 (01)FP, Contract NAS 9-4355, Apr. 1967.
3. Evaluation of Thermal Instrumentation for Project Fireball. Final report, Lockheed Electronics Company for Instrumentation and Electronic Systems Division of MSC. IESD Document No. 021-2, Feb. 1966.
4. Fago, E. T.; Klein, V. W.; and Moeller, C. E.: Determination of Transient Temperature During the Expansion of Fireballs. Midwest Research Institute Rept. 2885-E for Contract NAS 9-4448, Mar. 1966.
5. Lutzky, M.: The Flow Field Behind a Spherical Detonation in TNT Using The Landau-Stanyukovich Equation of State for Detonation Products. U. S. Naval Ordnance Laboratory Rept. NOLTR 64-40, Feb. 1965.
6. Gayle, J. B.; Blakewood, C. H.; Bransford, J. W.; Swindell, W. H.; and High, R. W.: Preliminary Investigation of Blast Hazards of RP-1/LOX and LH₂/ LOX Propellant Combinations. NASA TM X-53240, Apr. 1965.
7. Kingery, C. N.; and Pannill, B. F.: Peak Overpressure vs Scaled Distance for TNT Surface Bursts (Hemispherical Charges). BRL Memorandum Rept. 1518, Apr. 1964.
8. Mills, R. R.; Fish, F. J.; Jezek, B. W.; and Baker, W. E.: Self-Consistent Blast Wave Parameters. DASA-1559, Oct. 1964.
9. Kingery, C. N.: Air Blast Parameters vs Distance For Hemispherical TNT Surface Bursts. BRL Report No. 1344, Sept. 1966.